PASJ: Publ. Astron. Soc. Japan , 1–**??**,

A Study of Polar Jet Parameters Based on Solar-B XRT Observations

Antonia Savcheva, Jonathan Cirtain, Ed DeLuca, Loraine Lundquist, Leon Golub, Mark Weber,Jay Bookbinder
Harvard-Smithsonian CfA
60 Garden st., Cambridge, MA 02139
asavcheva@cfa.harvard.edu
jcirtain@cfa.harvard.edu
edeluca@cfa.harvard.edu
llundquist@cfa.harvard.edu
lgolub@cfa.harvard.edu
mweber@cfa.harvard.edu
jbookbinder@cfa.harvard.edu
and
Masumi Shimojo, Sakum Tsuneta, Kiyoto Shibasaki
Nobeyama Solar Radio Observatory/NAOJ/NINS, Japan
shimojo@nro.nao.ac.jp
saku.tsuneta@nao.ac.jp
Shibasaki@nro.nao.ac.jp
and
Taro Sakao, Noriyuki Narukage
ISAS/JAXA, Japan
Sakao.Taro@isas.jaxa.jp
narukage@solar.isas.jaxa.jp
and
Ryouhei Kano
NAOJ, Japan
ryouhei.kano@nao.ac.jp

(Received ; accepted)

Abstract

Hinode/SoHO campaign 7197 studied polar jet formation from within both the north and south polar coronal holes. Using the observations collected by the X-Ray Telescope on Hinode, a number of physical parameters of the jets have been statistically studied. In this work we show the results for the apparent outward and transverse velocity and measurements of the height, width and lifetime of the jets. These parameters show peaked distributions with maximums at 160 km/s for the outward velocity, 0 km/s for the transverse velocity, 50000 km for the height, 8000 km for the width, and about 10 min for the lifetime of the jets. We describe the methods used to determine these characteristics and set some future goals. We also show that despite some possible selection effects jet preferably occur inside the polar coronal hole.

Key words: Sun: corona, magnetic field

1. Introduction

In the early nineties the Yohkoh mission showed clearly that reconnection events, and more specifically jets, play an important part in coronal dynamics (Shimojo et al, 1996). One of the main goals underlying the launch of the X-ray telescope on board the Hinode satellite was to study magnetic reconnection in the corona by observing its different manifestations. With the advantage of the highest spatial resolution of any solar X-ray mission and a broad range of detectable temperatures, XRT is the perfect telescope for studying both the statistical properties of jet parameters and model individual events. In this work we concentrate on a statistical study of different jet parameters like apparent outward velocity, transverse velocity, width, maximum height, duration, and spatial distribution.

In November 2006, January 2007, and March 2007 XRT participated in an extensive study of reconnection events in both polar coronal holes. For the following analysis we use data taken during the January-2007 run of the SOHO/Hinode campaign 7197, which looked at the South pole coronal hole.

2. Observations

SOHO/Hinode campaign 7197 was run between January 08 and January 21, 2007. For 6-12 hours each of these days, XRT took high-cadence observations of the South pole coronal hole. Two different filters were used - each one taking data for 4-7 hours every day. The maximum of the temperature response of the aluminum polyamide filter is about 7 million degrees (with a significant peak at 1 million degrees as well) and that of the titanium polyamide one is close to 8 million. Time constraints allowed us to conduct our analysis only on images taken in the aluminum poly filter in the interval Jan 12 - Jan 19. All images are 1024×512 pixels or $1053' \times 526.6'$, and centered on the South pole.

Jet events were selected according to the following 2 conditions: The visible ejection of material happened on the timescale of several tens of minutes; an increase in the length of the brightening (associated with the jet) with time. After applying these conditions, all jet events are formed into a separate data subsets covering the time interval between the emergence of bright dipole, the reconnection event, and relaxation of the loop structure after the jet. Following these criteria, we produced a total of 104 subsets, covering time intervals between 5 min and 2 hours. All images were cut to a size of 20 pixels by 30-200 pixels.

On all data subsets we performed initial image preparation and cleaning techniques. All images were processed for different kinds of instrumental noise and cosmic particle hits. All data were also normalized by exposure time.

In figure 1, we have given an example of a jet that was observed in the aluminum poly filter at 13:11 UT on Jan 17-th. We have shown an image when the jet has reached maximum length, or as we call it later, height. The underlying loop structure is also well distinguishable.

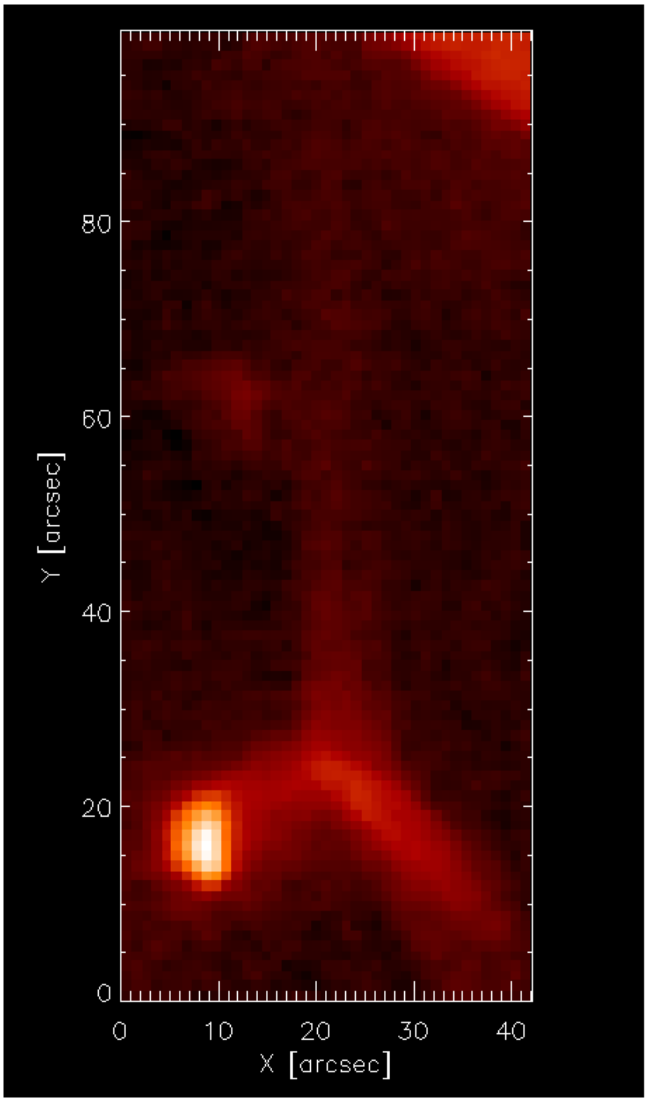

Fig. 1. Image of a polar coronal jet after the instrumental noise and cosmic particle hits have been removed. The image has also been normalized by exposure time and rotated vertically.

3. Outward velocity determination

The first parameter we worked on was the apparent outward jet velocity. While developing the methods for determining the velocity we were able to find better ways to post-process the images, so the subsequent analysis is carried out more rigorously.

3.1. Image processing

For some parts of the analysis certain image post-processing was necessary. After the image was initially processed, the cleaned and normalized image was smoothed using a Gaussian low-pass filter with $\sigma = 2$ pix. After that a Laplacian edge-detection filter was applied, consisting in taking the Laplacian of the Gaussian-smoothed image and adding it back to the smoothed image. This way, a considerably sharpened and denoised imaged was produced. In Fig 2, you can see the same frame as the one shown in Fig. 1, but after the post-processing just described.

3.2. Methods

Several different methods were developed for determining the jets apparent outward velocities. The first method we discussed was suggested before by ... (...) and we refer to it as the 'Stack plot' method. The next two methods use the same basic idea but with different variations. The fourth method relies on a different concept. While the first three methods give an estimate of the velocity associated with the evaporation flow in the jet, we believe that the last method gives us information mainly about flows happening on much faster timescales.

The first three methods give velocity estimates in the range 70 km/s to 400 km/s. This result is well consistent with previous statistical studies of jets (Shimojo 1996, Dobrzycka 2002). The last method sometimes detected higher velocities of about 600 km/s, but they were not included in the statistical analysis. On figure 3 you can see the velocity histogram distribution for 101 jets. The distribution peaks at about 160 km/s and bigger wing towards the higher velocities is well noticeable.

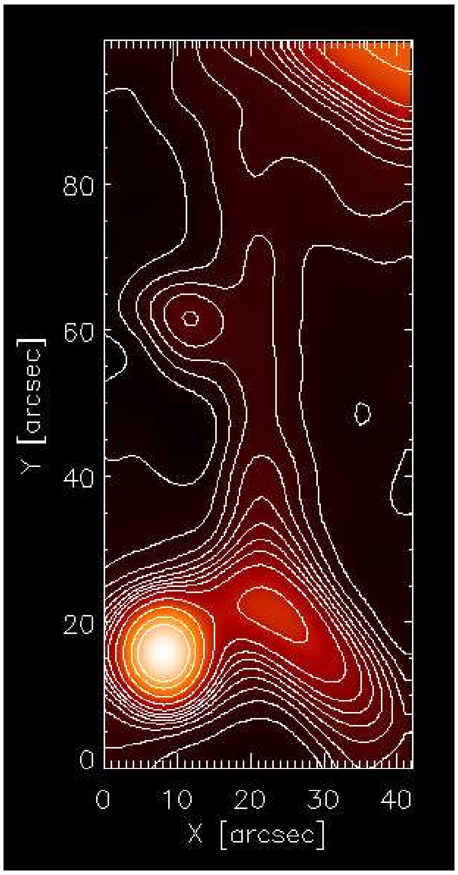

Fig. 2. The same image as shown on the previous figure after gaussian low-pass and Laplacian edge-detection filters have applied.

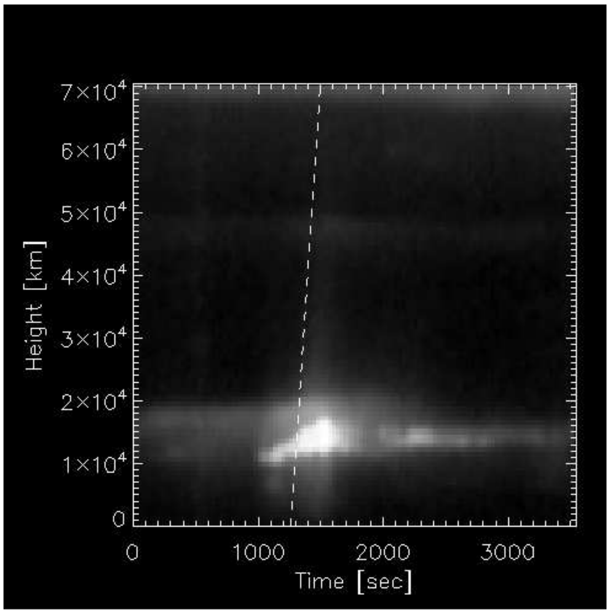

Fig. 3. This figure demonstrates the basic 'stack plot' method for velocity detrmination. A line ahas been fit to the left slope of the bright region.

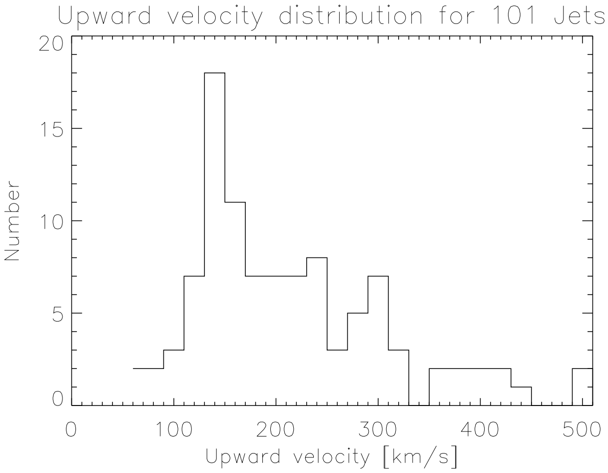

Fig. 4. Histogram distribution of upward jet velocities.

3.2.1. The 'Stack plot' method

We apply the following method on images in the form shown on Fig. 1. Here we do not make use of the post-processing techniques yet. The idea behind the method is the following: Consider an image consisting of n columns and m rows. If one sums over the n elements of a given raw one would get the width-averaged brightness at any distance from the base m. Thus, for a given time, we get single column to represent the whole image (Fig. 3). Plotting such column for every instance of the jet, we effectively produce a plot of brightness with height and time. Then, we fit a straight line to the left side of the bright region on the figure to obtain the apparent outward velocity of the jet. If we assign physical units of seconds and kilometers to the X- and Y- axis of this plot, we obtain the velocity in km/s.

This method proved useful for most of the brighter jets when the contrast between the jet and the background is relatively high. The error bar on the velocity given by this method (about 30 km/s) is somewhat higher that the one given by the other methods.

3.2.2. The 'Difference Stack plot' method

This method uses the same basic idea as the previous one in a sense that the result is a time-lapsed image where every column represents brightness of the jet with height at a given time. However, from each column we now subtract the forth column further away in time, thus producing a time-difference plot.

Such a plot has the advantage that it takes away almost all background, even spatial gradients which otherwise would require some more extensive modeling. The method also highly exaggerates the contrast between the jet and the background and makes it easier to select the slope from which to extract the velocity. This method also give smaller error bars (about 10-15 km/s), and it is probably more precise as well.

3.2.3. The Laplacian contour method

The method discussed here is a subsequent build-up on the 'Stack plot' method. It involves applying post-processing techniques onto the 'stack plot' image obtained as descried in 3.1.1. A Gaussian low-pass filter and a Laplacian operator are applied to the image plot. The image is scaled so that positive derivatives appear in white and negative - in black. The +/- contours are drawn and a part of a contour is selected, which represent the left slope of the jet. Choosing the contour so it does not crosses itself, we fit a line to it and obtain an estimate of the velocity.

This method works best for jets which outward flow appears uninterrupted by other brighter structures and when the background is fairly smooth. Used with jets with the right conditions, this method gives smallest errors - about 5-10 km/s and also involves least judgment from the person processing the data.

3.2.4. The brightness contour method

The brightness contour method is developed on the basis of an entirely different concept. Here, we consider every image of the jet from its data subset and process to the level after the Laplacian edge-detection filter. We then draw isocontours of different brightness levels. To determine the velocity we just plot the vertical position of the maximum of a given contour with time and fit a line to it. We secure the fact that the maximum of the contour may not behave perfectly by choosing another four equally-spaced along the contour points.

In some cases this method gave consistent results with the other three methods, although sometimes the error bars were very big. In the rest of the cases the velocities it yielded were systematically higher - up to 600-700 km/s. As explained above, we think that the different nature of the method, and more specifically the fact that it does not uses averaging along the width of the box, actually gives us an insight into a different process, which we plan to examine in another work.

One would say that this method seems more straightforward, but we wanted to explore different methods which are suitable for different jet events. We chose to discuss this method last because all other parameters we study are derived from the same type of contour analysis.

4. Other jet parameters

4.1. Heights

We base the determination of the jet lengths, or heights, on the contour method described above. Apparently, we first have to define where the end of the jet is in height. We simply define the jet to be confined in a brightness contour of a given value. This value is chosen with respect to a reference jet by the following formula $C = C_{ref}\frac{J-B}{J_{ref}-B_{ref}}$. Here C, J, B are the contour value, the jet brightness in the moment of maximum height, and the background brightness for the event at hand, and C_{ref}, J_{ref}, and B_{ref} are the same ones for the reference jet. After we have done this, we simply follow the vertical position of a given brightness contour with time and record its maximum values.

The height derived that way are all in the range $10^4 - 1.2\times10^5$ km/s, which is consistent with previous statistical and model-oriented studies done on jets (Shimojo et al, 1996). On Fig. 5 we have shown the distribution of height for 102 jets. The times of moment of maximum height was recorded and it will be used as a parameter in future work concentrating more on the physical picture, rather than the statistical properties of jets.

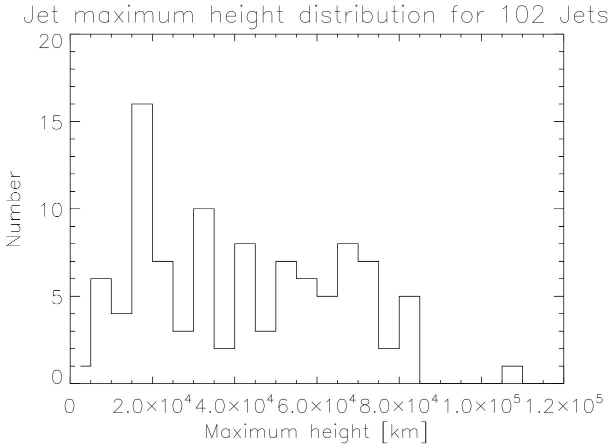

Fig. 5. Histogram distribution of jet maximum heights.

4.2. Collimated widths

Along with the jets heights, we calculated the widths of the jets at several different heights. Of course, the calculation for any width is the same, but in this study we consider only the height-average width of the jet above a certain height. We decided to do that, since many authors have noticed that jets appear to be highly collimated after certain height. We determine these collimated widths.

For a cross-section at a given height, the width of the jet is calculated in the following way: $\omega = \sqrt{<x^2> - <x>^2}$ with x being the position in the transverse direction in pixels. In order to calculate the terms on the RHS, we just need to normalize the brightness distribution so it has the form of a probability. We calculate it as $p(x) = \frac{b(x)-b_{backgr}}{\sum_x(b(x)-b_{backgr})}$, where $b(x)$ and b_{backgr} are blitheness of the jet and the background. Since this calculation is done on the Gaussian smoothed image, we then apply small correction to the result, taking into account variance of the Gaussian used for smoothing.

The result of this calculation was that jets lye well in the range between 6000 km and 10000 km with just a few exceptions. In Fig. 6 you can see the histogram distribution of jet collimated widths for all 104 jets. A more thorough analysis of the distribution of widths with height will be carried later in another work.

4.3. Transverse velocities

While working on the other characteristics, we noticed that most jets exhibit a substantial transverse motion, along the underlying loop structure in the plane of the sky. We calculated these velocities in the same way we calculated the outward velocities using the brightness contour method. We looked at the motion of the maximum of a given contour in the transverse direction with time and

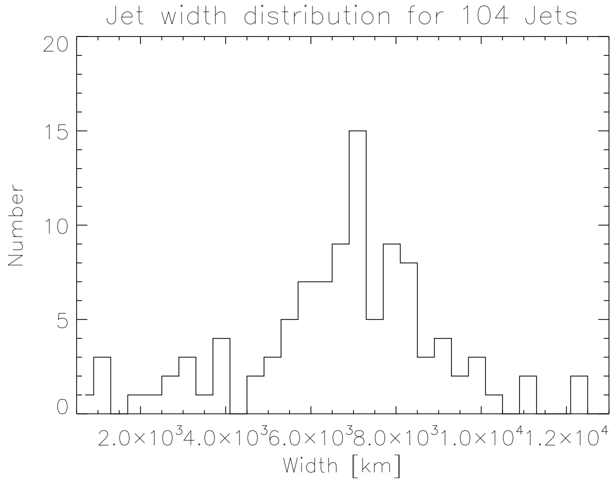

Fig. 6. Histogram distribution of jet widths.

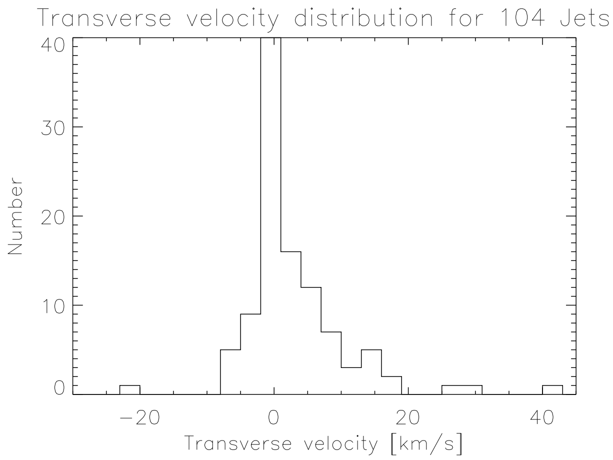

Fig. 7. Histogram distribution of jet transverse velocities. The peak at 0 km/s is artificially high since the transverse velocities around 0 km/s of many jets have large uncertainties.

fitted a line to it.

The transverse velocities vary between 0 - 35 km/s. In the figure we have shown the distribution of transverse velocities. Note that the peak at 0 km/s is artificially high since some jets have too big error bars around 0 km/s. We observed that most of the closed field structures in the coronal hole were oriented in the East-West direction and hence the jet apparent transverse velocities were also in the East or West direction. On the figure, negative velocities are pointing to the West and positive are to the East, centered at 0 km/s.

4.4. Lifetimes

The lifetimes of the jets were also a characteristic which was easily determined, at no cost, in the process of estimating other parameters. We defined the beginning of the jet to be the moment when a little spike of brightness starts emerging from the reconnection site and becomes visible. Similarly, the end of the jet was set to be the moment when no elongation is present. All these moments were determined in a not very rigorous way - by eye. Being consistent with our initial criterion for a jet event, most jets proved to last for several minutes to several tens of minutes. It can be seen from the histogram plot below that jet lifetimes peak at about 10 min.

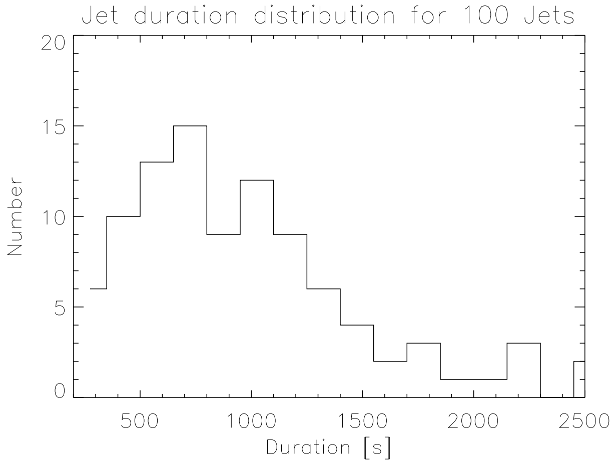

Fig. 8. Histogram distribution of jet durations.

5. Jets and the polar coronal hole

While making the data subsets for every jet we obtain information about the position of the jets in pixel coordinates. We then fit the limb of the sun to all images containing jets and extract the heliocentric coordinates of the origin of the jet stream. We then chose an image from the Jan 19 and rotated all jet positions to this time. We plot the rotated position onto a representation of the solar disk looked from the South pole (Fig. 7). As it was expected all jets were confined near the South pole in one E-W hemisphere.

We also extract the boundary of the South pole coronal hole as seen in the aluminum poly on the 17-th and rotate it to the same time as the jets were rotated to. After we plot the boundary of the coronal hole on the same plot (Fig. 7) we see that all observed jets fall strictly inside the boundary of the coronal hole. We do not exclude the possibility for an observational selection effect coming from the fact that the background level in the coronal hole is much less than outside it and jets there are much easier to spot. In any case, we believe that such a selection effect cannot count against a more even spatial distribution of jets across the coronal hole boundary.

We also plot jet apparent outward and transverse velocities symbol-coded with the positions. On Fig. 7 slower jets - with velocities ¡ 160 km/s are plotted with asterisk, and faster jets - with velocities ¿ 160 km/s are plotted with triangles.

On Fig. 8 jets with positive velocities are plotted with pluses, and jets with negative velocities - with diamonds. Both spatial distribution show no obvious dependence of the value of the velocity on the jet position relative to the

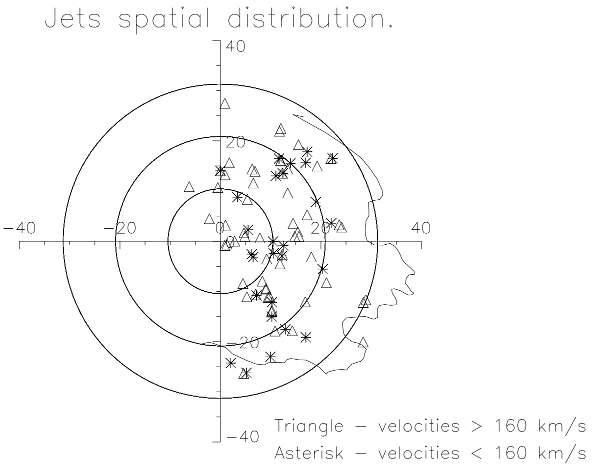

Fig. 9. Jets positions on the solar disk. Jet velocities are symbol-coded to show the distribution of upaward velocities with position. The boundary of the poalar coronal hole is also shown.

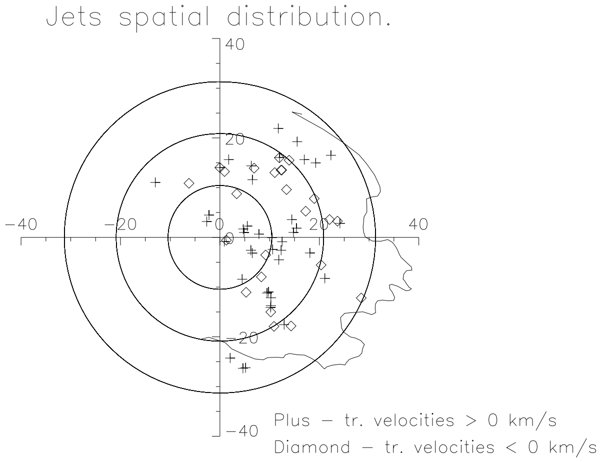

Fig. 10. Jets positions on the solar disk. Jet transverse velocities are symbol-coded to show the distribution of these velocities with osition. The boundary of the poalar coronal hole is also shown.

coronal hole boundary.

6. Conclusion

Here we presented a statistical study of different jet parameters conducted on the data collected during the Hinode/SoHO campaign 7197 in January 2007. For the determination of the apparent outward velocity we developed four methods. We obtained that the histogram distribution for the apparent outward velocity of the jets peaks at about 160 km/s. We also derived that the transverse velocity, height, width, and lifetime have mean values of about 0 km/s, 50000, 8000 km, and about 10 min respectively. We also demonstrated that most jets are situated inside the polar coronal hole.

During this study, some interesting events were selected and more thorough analysis of the parameters discussed above as well as other characteristics will be studied in an attempt to constrain the model for jet events.

References

Dobrzycka, D., Cranmer, S.R., raymond, J.C., Biesecker, D.A., Gurman, J.B. 2002, ApJ, 565, 621

Shimojo, M., Hashimoto, S., Shibata, K, Hirayama, T, Hudson, H., Acton, L. 1996, PASJ,48, 123

Aauthor, A., Bauthor, B. 2001, Name of Book(Publisher, Tokyo) page0 ......

Dauthor A. A. 2001, in Name of Book, ed Editor D. Editor(Publisher, Tokyo) page0